

Robust Machine Learning for Regulatory Sequence Modeling under Biological and Technical Distribution Shifts

Yiyo Yang

yy3555@tc.columbia.edu

ORCID: 0009-0001-8693-4888

Columbia University, New York, NY, United States

I. Abstract

Robust machine learning for regulatory sequence modeling is examined under biologically and technically induced distribution shifts. Although deep convolutional and attention-based architectures achieve strong in-distribution performance on regulatory tasks, they are predominantly evaluated under i.i.d. assumptions, despite deployment contexts involving cell-type-specific regulatory programs, evolutionary turnover, assay protocol differences, and sequencing artifacts. A robustness framework is introduced combining a mechanistic simulation benchmark with real-data evaluation on a massively parallel reporter assay (MPRA) dataset to characterize performance degradation, calibration failures, and uncertainty-based reliability mechanisms. In simulation, motif-based regulatory outputs are generated with cell-type-specific programs, PWM perturbations, GC-dependent biases, depth variation, batch effects, and heteroscedastic noise. CNN-, BiLSTM-, and transformer-based models are then assessed. Models remain accurate and reasonably calibrated under mild GC-content shifts but exhibit 2–10× higher error, severe variance miscalibration, and interval coverage collapse under motif-effect rewiring and noise-dominated regimes, revealing a robustness gap not captured by standard IID evaluation. Introducing simple biological structural priors—motif-derived features in simulation and global GC-content in MPRA, improves in-distribution error and yields consistent robustness gains under biologically meaningful shifts, while offering only limited mitigation under strong assay noise. Uncertainty-aware selective prediction further provides a practical mechanism for enhancing reliability: risk-coverage analyses on both simulated and MPRA data show that filtering low-confidence inputs recovers low-risk subsets, including under GC-based out-of-distribution conditions, although reliability gains diminish when aleatoric noise dominates. Overall, the findings highlight the need to evaluate regulatory sequence models not only on IID accuracy but also on robustness, calibration, and uncertainty when facing realistic genomic distribution shifts.

II. Introduction & Literature Review

Understanding how DNA sequence encodes regulatory function is a central problem in computational genomics, with downstream applications in enhancer mapping, variant interpretation, and disease genetics (Gasperini et al., 2019). Recent progress in deep learning, especially convolutional architectures and attention-based models capable of integrating long-range genomic context, has substantially advanced predictive accuracy on regulatory tasks, such as chromatin accessibility, TF binding, and gene expression prediction from raw sequence (Zhou & Troyanskaya, 2015; Agarwal & Shendure, 2020; Avsec et al., 2021). While these sequence models are increasingly used as components in scientific and clinical pipelines, their evaluations overwhelmingly rely on in-distribution metrics and i.i.d. assumptions. In reality, regulatory genomics is fundamentally non-i.i.d.: biological variability and technical variation induce structured distribution shifts relative to the training distribution. When such models are used to prioritize genetic variants or impute regulatory activity in unmeasured tissues, robustness and uncertainty become essential for reliable interpretation. However, despite growing adoption, the robustness properties of regulatory sequence models remain largely unexplored.

Early deep learning approaches framed regulatory prediction as sequence-to-output classification or regression tasks, using convolutional neural networks to infer TF binding, chromatin accessibility, and histone modifications from raw DNA sequence (Zhou & Troyanskaya, 2015; Kelley et al., 2016; Alipanahi et al., 2015). Subsequent work extended convolutional architectures to longer genomic context (Agarwal & Shendure, 2020; Kelley, 2020), while attention-based models further improved long-range interaction modeling and variant effect prediction (Ji et al.,

2021; Avsec et al., 2021). These architectures demonstrated strong performance on benchmarks involving chromatin state imputation, enhancer prioritization, and fine-mapped eQTL interpretation.

Beyond predictive accuracy on epigenomic tracks, sequence models have also been applied to downstream tasks such as enhancer–promoter interaction inference (Fulco et al., 2019; Gasperini et al., 2019), saturation mutagenesis and massively parallel reporter assays for mutation effect estimation (Rentzsch et al., 2018), and causal variant prioritization in GWAS and fine-mapping studies (Weissbrod et al., 2020; Wang et al., 2021). These applications highlight an emerging role of sequence-based models as computational surrogates for experimental assays, with potential to guide experimental design and clinical variant interpretation.

Despite this progress, existing evaluations predominantly consider i.i.d. settings, typically using random genomic splits or held-out chromosomes for in-distribution generalization. In contrast, realistic regulatory genomics scenarios involve substantial distribution shifts: cell-type-specific regulatory programs (Heinz et al., 2010), species divergence and evolutionary turnover of enhancers (Villar et al., 2015), assay protocol and readout differences (e.g., DNase-seq vs. ATAC-seq), and sequencing-specific technical artifacts such as depth variability and batch effects. From a machine learning perspective, these represent domain shift, covariate shift, and structured OOD problems that are widely studied in vision and language (Quionero-Candela et al., n.d.), yet largely unaddressed in regulatory genomics.

Similarly, while uncertainty quantification and calibration have become central in ML for high-stakes decision-making, via Bayesian approximations (Gal & Ghahramani, 2015), ensembling (Lakshminarayanan et al., 2017), and selective prediction, analogous methods for genomic sequence models remain underexplored. Existing regulatory modeling studies rarely examine calibration, robustness under OOD conditions, or selective prediction performance, despite the increasing use of model outputs for variant prioritization and downstream interpretation.

Taken together, current sequence-based regulatory models excel in predictive accuracy but lack systematic assessment and mitigation of robustness, uncertainty, and reliability under biological and technical distribution shifts. This gap motivates the need for a principled robustness framework tailored to regulatory genomics.

III. Research Questions

Research Question 1: To what extent do current regulatory sequence models preserve predictive performance and calibration under biologically and technically induced distribution shifts?

Research Question 2: Can incorporating biological structural priors improve robustness under distribution shift without degrading in-distribution performance?

Research Question 3: Can uncertainty estimation and selective prediction provide biologically meaningful safety mechanisms when regulatory sequence models encounter out-of-distribution (OOD) genomic conditions?

IV. Research Techniques & Programming Tools

The programming language used in this study is Python. For each research question, the computational methods and Python libraries across research questions (Table 1), ranging from sequence-to-function convolutional architectures and PWM-based structural priors to uncertainty-aware selective prediction, alongside the corresponding Python libraries used for implementation, evaluation, and visualization. The summary makes the computational workflow and software stack transparent and supports reproducibility of the presented analyses.

Table 1*Computational Methods and Python Libraries Across Research Questions*

Research Questions	Techniques Used	Python Libraries
Performance & Calibration under Shifts	<ul style="list-style-type: none"> - Sequence-to-function modeling (CNN) - Biological covariate shifts (GC) - Technical shifts (noise) - Regression metrics (MSE) - Calibration evaluation (ECE) 	<ul style="list-style-type: none"> - PyTorch (CNN regression & classification) - Scikit-learn (performance metrics) - Numpy (GC-biased sequence simulation & array operations) - SciPy (Gaussian quantiles for coverage) - Matplotlib & Seaborn (performance and calibration plots)
Structural Priors for Robustness	<ul style="list-style-type: none"> - CNN + PWM structural priors - Sequence-motif feature fusion - Heteroscedastic Gaussian regression - Robustness evaluation across genomic shifts - Variance calibration (Var-ECE, coverage) 	<ul style="list-style-type: none"> - PyTorch (model architecture) - Numpy (data processing) - Scikit-learn (evaluation metrics) - Matplotlib & Seaborn (visualization)
Uncertainty & Selective Prediction	<ul style="list-style-type: none"> - Heteroscedastic variance-based uncertainty - Confidence-based selective prediction (risk-coverage) - Selective risk analysis (regression and classification) - Robustness under biological and technical OOD shifts - Selective abstention across shifts 	<ul style="list-style-type: none"> - PyTorch (CNN baseline model and batch inference) - NumPy (uncertainty-based coverage filtering and sample ranking) - Scikit-learn (classification accuracy and risk estimation) - Matplotlib and Seaborn (risk-coverage curves and heatmap visualizations for regression and classification)

Note. Programming Language: Python

V. Simulated Regulatory Benchmark

To investigate robustness properties of regulatory sequence models under well-controlled distribution shifts, we construct a simulated benchmark that captures key biological and technical mechanisms driving gene regulation while enabling systematic variation across domains. In contrast to real-world genomics datasets, where biological and technical factors are intertwined, and ground-truth uncertainty is unobservable, our simulation framework offers explicit control over cell-type-specific regulatory logic, configurable technical perturbations, and observable heteroscedastic noise for calibrating uncertainty methods. This design allows principled stress-testing of robustness, uncertainty, and selective prediction under controlled shifts.

Regulatory Sequence Generation

We simulate a DNA sequence $x \in \{A, C, G, T\}^L$ of fixed length $L = 1000$. Background nucleotides are sampled from a GC-biased distribution reflecting variable chromatin composition:

$P(A) = P(T) = \frac{1-g}{2}$, $P(C) = P(G) = \frac{g}{2}$ where $g \in [0, 1]$ controls GC-content and can later induce GC-related technical shifts.

Motif-Based Regulatory Activity

We define K a transcription factor (TF) motif $\{M_k\}_{k=1}^K$, simulated as position weight matrices (PWMs).

For each sequence, motif occurrences contribute additive activation:

$$a_k(x) = \sum_{t=1}^{L-|M_k|+1} I[x_{t:t+|M_k|-1} = M_k] \cdot w_k, \text{ where } w_k > 0 \text{ represents motif affinity strength.}$$

This modeling choice reflects regulatory logic observed in enhancer sequences, in which the presence and multiplicity of TF binding motifs contribute to regulatory output.

Cell-Type-Specific Regulatory Logic

To simulate biologically meaningful variation, we define C cell types with TF activity coefficients $\alpha_{c,k}$.

Regulatory output for cell type c is: $z_c(x) = \sum_{k=1}^K \alpha_{c,k} a_k(x)$.

We consider two readout regimes:

Continuous: $y_c(x) = z_c(x) + \epsilon_c$, $\epsilon_c \sim N(0, \sigma_c^2(x))$

Binary: $y_c(x) = I[z_c(x) > \tau_c]$

Since $\sigma_c(x)$ varies by motif content, the continuous regime enables heteroscedastic uncertainty, it is essential for calibration experiments.

Biological Distribution Shifts

We simulate biological OOD scenarios by varying TF activity coefficients across train/test cell types. Let training cell types be C_{train} , and OOD test cell types be C_{test} , with $C_{train} \cap C_{test} = \emptyset$.

We sample TF activities as: $\alpha_{c,k}^{test} \sim N(\alpha_{c,k}^{train}, \sigma_{bio}^2)$, where σ_{bio} the control biological domain shift magnitude. Larger σ_{bio} corresponds to stronger tissue-specific regulatory divergence analogous to GTEx multi-tissue expression variation.

We further simulate motif evolution via PWM perturbations: $M_k^{test} = T(M_k^{train}, \delta)$, where substitution probability δ mimics enhancer turnover across species.

Technical Distribution Shifts

Technical variation is simulated independently of biological logic:

(1) Sequencing Depth Shift: We apply multiplicative noise: $\tilde{y}_c = y_c \cdot d$, $d \sim \text{LogNormal}(\mu_d, \sigma_d^2)$, modeling read-depth variation in ATAC-seq/RNA-seq.

(2) Batch Effects: We add nuisance offsets: $\tilde{y}_c = y_c + b$, $b \sim N(0, \sigma_b^2)$ capturing between-batch variability in high-throughput assays.

(3) GC-Bias: We distort output based on GC-content: $\tilde{y}_c = y_c \cdot (1 + \beta(GC(x) - \mu_{GC}))$, reflecting GC-dependent mapping efficiency commonly observed in sequencing pipelines. Together, these perturbations simulate covariate shift, label shift, and spurious correlations frequently seen in functional genomics.

Structured Perturbations: To evaluate post hoc robustness, we introduce targeted edits, including motif knockout (remove motif occurrences $\Delta M = 0$), motif insertion (adds strong binding sites), TF rewiring (permutes $\alpha_{c,k}$ across TFs), and motif masking (emulates epigenetic silencing). These simulate enhancer deletions, gain-of-function mutations, or chromatin rewiring events observed in saturation mutagenesis and MPRA assays.

Model Architectures: We evaluate three representative architectures, including the CNN-based regulatory model (modeling local motif detection), the BiLSTM-based model (capturing mid-range motif dependencies), and the Transformer-based long-range model (inspired by Enformer architecture and capable of long-range attention). The transformer uses sinusoidal positional encodings and multi-head attention, but is adapted to reduced sequence lengths to match the simulation scale.

Evaluation Metrics: We evaluate models along three axes aligned with our research questions:

In the RQ1 (Performance under Distribution Shift), the evaluation metrics include In-Distribution (ID) accuracy, Out-Of-Distribution (OOD) accuracy, worst-group accuracy, and Domain Gap $\Delta = ID - OOD$. In the RQ2 (Structural Robustness), the evaluation metrics include Motif Perturbation Sensitivity and TF-Rewiring Stability. In the RQ3 (Uncertainty & Selective Prediction), we quantify uncertainty via Predictive Entropy, MC Dropout Variance, and Deep Ensemble Variance. Calibration is measured using Expected Calibration Error (ECE), Negative Log-Likelihood (NLL), and Brier Score. Selective prediction is evaluated via risk-coverage curves:

$$R(c) = E[\ell(f(x), y) \mid u(x) \geq u_c], \text{ where } u(\cdot) \text{ is uncertainty, and } c \text{ is retained coverage.}$$

Simulation Summary: Taken together, this simulated benchmark provides a controlled yet biologically inspired environment for robustness evaluation. By explicitly parameterizing biological variability (via cell-type-specific regulatory programs and motif evolution), technical perturbations (including depth shifts, batch effects, and GC-bias), and ground-truth heteroscedastic uncertainty, it offers clear and tunable OOD scenarios grounded in realistic motif-based regulatory logic. This design enables comprehensive and interpretable assessment of robustness, calibration, and selective prediction, without the confounding experimental artifacts and unobserved factors that complicate analyses on real-world genomics data.

VI. Data Analysis & Result

(VI.1) Performance on Simulated Dataset

Research Question 1: Evaluating Robustness Under Genomic Distribution Shifts

To quantify robustness, we evaluated a heteroscedastic Gaussian CNN and a derived binary classifier under a suite of biologically and technically motivated distribution shifts, including GC-content covariate shift, heteroscedastic assay noise, motif–effect rewiring (concept shift), and their combination (Figure 1). On in-distribution test data (Figure 2), the regression model achieved low error (MSE ≈ 0.10) with well-calibrated variance estimates (Var-ECE ≈ 0.03 , 90% coverage ≈ 0.85). Mild GC-content shifts produced only marginal degradation (MSE ≈ 0.11 , Var-ECE ≈ 0.04), indicating that shallow sequence-level perturbations alone are not major failure modes.

Figure 1

Regression MSE Under Distribution Shifts

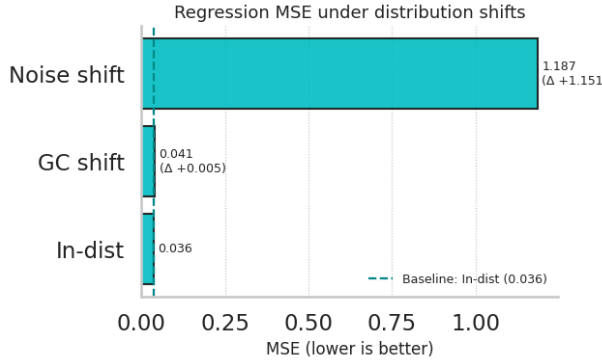
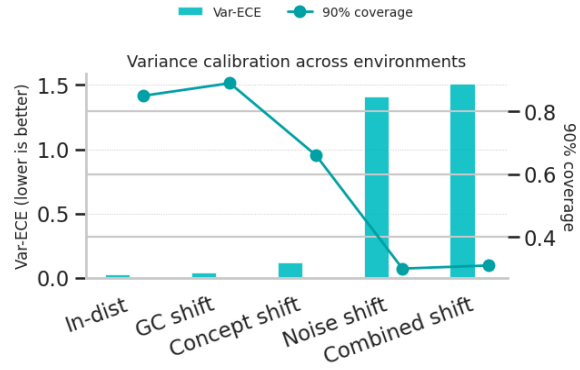


Figure 2

Variance Calibration Across Environments



On in-distribution test data (Figure 3), predicted mean activity closely tracks the true response, with points concentrated along the $y = x$ diagonal (Pearson $r = 0.96$), indicating that the Gaussian regression model achieves a strong baseline fit before any distribution shift is introduced (Figure 4).

Figure 3

Responses on the In-Distribution Test Set

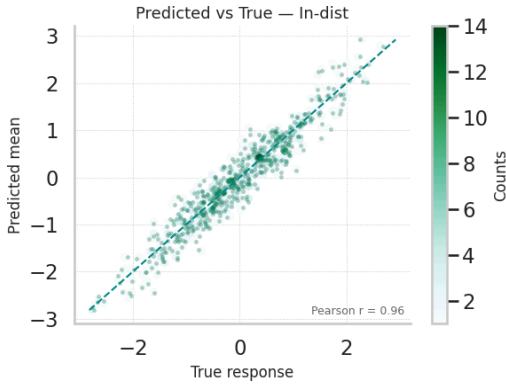
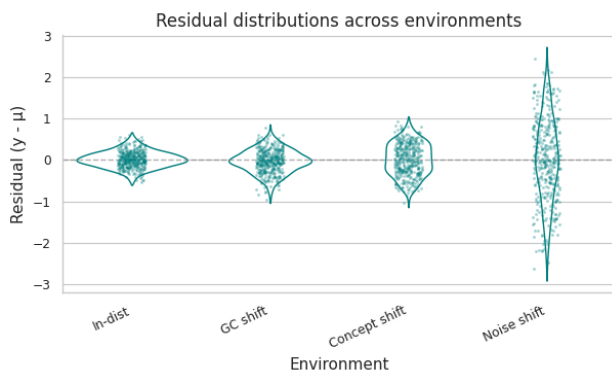


Figure 4

Residual Distributions



In contrast, both concept shift and technical noise induced substantial deterioration: motif–effect rewiring increased error by $2\times$ (MSE ≈ 0.21) and reduced interval coverage to 0.66, while heteroscedastic assay noise led to $>10\times$ higher error (MSE ≈ 1.50) and severe uncertainty underestimation (Var-ECE ≈ 1.41 , coverage ≈ 0.30). The combined shift produced the most pronounced collapse across metrics (MSE ≈ 1.63 , Var-ECE ≈ 1.51). A binary classifier trained on the same embeddings exhibited similarly shift-sensitive behavior, with accuracy fluctuating near chance (0.47 – 0.58) and ECE sharply increasing under concept shift (ECE ≈ 0.34). Taken together, these results

show that current regulatory sequence models preserve performance and calibration under shallow covariate shifts, but become systematically overconfident and error-prone under biologically meaningful mechanism shifts and realistic experimental noise, revealing a robustness gap not captured by standard IID evaluation.

From a biological standpoint, GC-content variation reflects compositional heterogeneity across genomic regions and species, which influences nucleosome occupancy and TF accessibility and also introduces assay-specific biases in PCR and sequencing. Motif–effect rewiring corresponds to the context-dependent nature of TF binding, where co-factors, chromatin state, and cell-type programs alter regulatory logic without changing the underlying DNA sequence. Heteroscedastic noise mirrors experimental uncertainty in regulatory assays such as ChIP-seq, DNase-seq, and ATAC-seq, where coverage, background signal, and biochemical efficiency generate input-dependent noise profiles. These perturbations capture realistic sources of distribution shift in regulatory genomics.

Research Question 2: Structural-Prior Gaussian Regression

To incorporate biologically meaningful inductive bias into the regression model, we augment sequence-based CNN representations with motif-derived structural priors. Given an input DNA sequence x , we first compute a vector of motif activation scores $m = f_{PWM}(x) \in R^K$ using a bank of PWMs, where each m_k summarizes the match strength of a motif k . In parallel, the raw sequence x is processed by a one-dimensional convolutional encoder, yielding a representation $h_{seq}(x) = \phi_{CNN}(x) \in R^{d_{seq}}$.

The motif scores are passed through a small MLP to obtain a structural embedding

$$h_{motif}(m) = \psi(m) = \sigma(W_m m + b_m) \in R^{d_{motif}}. \text{ The two components are then fused via concatenation:}$$

$h(x, m) = [h_{seq}(x) | h_{motif}(m)] \in R^{d_{seq} + d_{motif}}$, enabling the model to integrate both generic sequence patterns and biologically grounded motif structure. On top of the fused representation, we place a heteroscedastic Gaussian head that outputs the conditional mean and variance:

$$\mu(x, m) = W_\mu h(x, m) + b_\mu, \log\sigma^2(x, m) = W_\sigma h(x, m) + b_\sigma, \text{ yielding the predictive distribution}$$

$$y | x \sim N(\mu(x, m), \sigma^2(x, m)).$$

The model is trained end-to-end by minimizing the negative log-likelihood:

$$L_{NLL} = \frac{1}{2} \left(\frac{(y - \mu(x, m))^2}{\sigma^2(x, m)} + \log\sigma^2(x, m) + \log(2\pi) \right),$$

which encourages both accurate predictions and well-calibrated uncertainty. This formulation encodes PWM-based biological priors directly into the predictive pathway while preserving the flexibility of the CNN encoder, allowing the model to leverage motif-level regulatory structure without constraining its capacity to learn additional sequence determinants.

Incorporating motif-based structural priors yields a strictly better in-distribution baseline and improves robustness to biologically meaningful GC and concept shifts: compared to the unconstrained Gaussian CNN, the structural-prior model achieves consistently lower MSE, tighter variance calibration, and empirical coverage that is closer to the nominal 90% level, especially under concept shift. Under severe heteroscedastic noise, however, the gains are modest, the structural-prior model largely inherits the same failure modes as the baseline, with MSE and variance

ECE remaining high and coverage far below nominal. Thus, structural priors can enhance robustness under distribution shift without degrading in-distribution performance, but they do not fully resolve robustness breakdowns driven by assay-level heteroscedastic noise.

Across environments, the structural-prior Gaussian CNN consistently matches or outperforms the baseline in terms of regression error (Figure 5). On the in-distribution test set, adding motif-based priors slightly lowers MSE (0.103 to 0.093), confirming that incorporating biological structure does not degrade IID performance. Under biologically meaningful distribution shifts, the gains become more pronounced: the structural-prior model reduces error under GC-content shift (0.107 to 0.087) and under motif-effect rewiring (0.209 to 0.184), indicating improved robustness when the underlying regulatory logic changes. In contrast, under severe heteroscedastic assay noise and the combined shift, both models exhibit large errors, and structural priors yield only modest improvements (1.498 to 1.481 and 1.628 to 1.549, respectively), suggesting that architectural priors alone are insufficient to counteract strong technical noise. Together, these patterns support that structural priors can enhance robustness to biological shifts without sacrificing in-distribution accuracy, but they do not fully resolve noise-driven failure modes.

In terms of calibration, structural priors yield clear benefits under biological regime shifts but do not eliminate failures under technical noise (Figure 6). On in-distribution data, the structural-prior model achieves both lower variance calibration error (Var-ECE: 0.028 to 0.007) and closer-to-nominal interval coverage (0.85 to 0.90), indicating that structural information helps the model quantify uncertainty more accurately without sacrificing fit. These improvements persist under GC-content shift, where Var-ECE remains low (0.040 to 0.007), and empirical 90% coverage stays tightly aligned with the target level. Under concept shift, structural priors again reduce miscalibration (0.122 to 0.094) and partially restore coverage (0.67 to 0.72), suggesting that biologically informed feature fusion helps the model maintain well-calibrated variance estimates when the regulatory logic changes. In contrast, under heteroscedastic assay noise and combined shifts, both models become severely miscalibrated (Var-ECE ≥ 1.39) and under-cover (≈ 0.30), indicating that structural priors alone cannot correct for strong technical noise that corrupts the observation process rather than the regulatory mapping itself. Collectively, these results show that structural priors enhance calibration robustness in biologically meaningful settings but leave noise-driven uncertainty failures largely unresolved.

Figure 5

Regression MSE: Baseline vs Structural-Prior

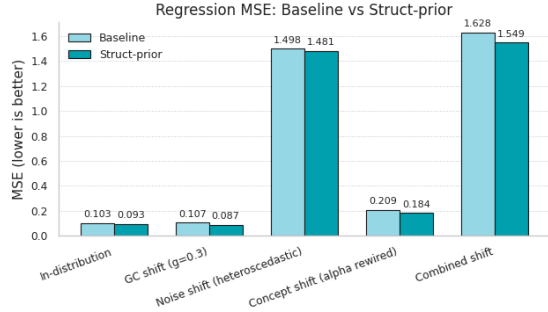
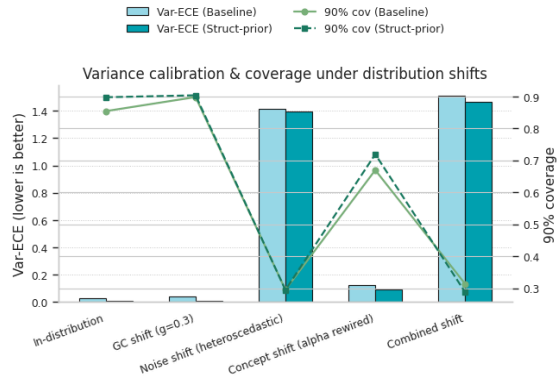


Figure 6

Variance Calibration & Coverage Under Distribution Shifts



Research Question 3: Uncertainty-Aware Selective Prediction as an OOD Safety Mechanism

To evaluate whether uncertainty estimates can provide selective safeguards under OOD conditions, we analyzed regression risk–coverage behavior across all distribution shifts (Figure 7). Under in-distribution test conditions and

mild GC-content covariate shift, the model exhibits a clean monotonic trend: restricting predictions to the most confident 10–30% of samples yields substantially reduced error (MSE \approx 0.10 to 0.06), indicating that predictive variance meaningfully correlates with estimation accuracy in these settings. Under biological mechanism shift (motif–effect rewiring), selective prediction remained partially effective, with low-coverage subsets achieving risk levels close to the in-distribution regime (MSE \approx 0.18), despite elevated full-coverage error. In contrast, under heteroscedastic assay noise and combined shift, risk–coverage curves flatten and remain $\gg 1.3$ MSE even at low coverage, revealing that aleatoric-dominated shifts destroy the coupling between uncertainty and correctness. These results suggest that uncertainty-aware selective prediction provides a practical safety mechanism against mild covariate and mechanism shifts, but offers limited protection under high-variance technical noise typical of real assays.

Selective prediction can indeed provide meaningful safeguards under biologically realistic OOD settings when uncertainty remains informative. Under concept shift (Figure 8), both models demonstrate the canonical risk–coverage pattern: constraining predictions to the most confident 10–30% of samples substantially reduces regression error, indicating that predictive variance correlates with correctness even when regulatory logic changes. However, the structural-prior model yields consistently lower risk at every coverage level (\approx 0.17 to 0.19 MSE vs. \approx 0.21 to 0.22 for baseline), demonstrating that motif-informed representations not only improve robustness overall but also strengthen uncertainty-based abstention strategies. These results suggest that uncertainty can act as a selective filter that preserves model reliability under mechanism shifts, and biologically grounded priors enhance the utility of uncertainty-guided safeguards rather than degrading them.

Figure 7

Regression Risk-Coverage Under Distribution Shifts

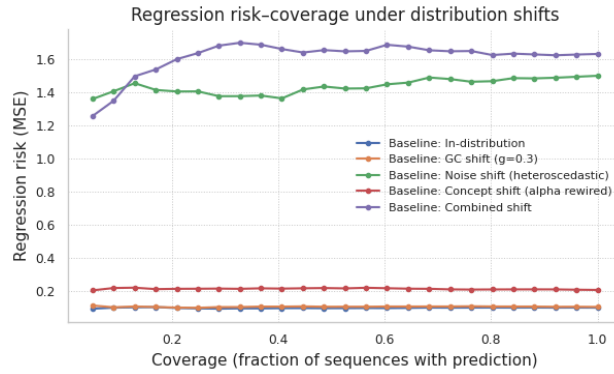
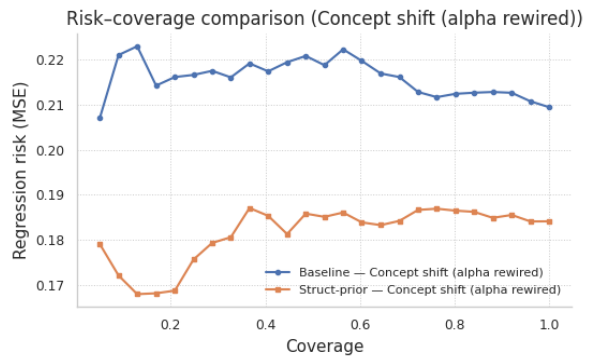


Figure 8

Risk-Coverage Comparison (Concept Shift)



To examine whether uncertainty can support reliable abstention in the binary setting, we computed risk–coverage curves for classification under the same suite of distribution shifts (Figure 9). Across all environments, the curves exhibit the expected monotone pattern: restricting predictions to the most confident 10–30% of samples reduces misclassification risk, indicating that predictive confidence retains some informativeness even under covariate, mechanism, and technical shifts. However, the strength of this effect is highly shift-dependent. Under in-distribution and GC-content shifts, selective prediction yields modest gains, reflecting that classification accuracy is already reasonably stable. Under concept shift, selective abstention is more impactful: risk drops from 0.42 at full coverage to 0.13 at low coverage, suggesting that confidence still partially tracks correctness even when regulatory logic is rewired. By contrast, under heteroscedastic noise and the combined-shift regime, selective filtering offers only limited robustness. Risk remains high (> 0.5) across coverage levels, indicating that confidence becomes poorly calibrated when assay noise fundamentally alters the signal-to-noise structure. For binary regulatory decisions, uncertainty remains a useful quality-control signal under genomic covariate and mechanism shifts, but fails to flag

unreliable calls when assay-level noise overwhelms the underlying sequence signal. Taken together, these results show that uncertainty-based abstention can function as a practical safeguard under biologically meaningful mechanism shifts, but it becomes insufficient when OOD conditions are dominated by severe technical noise that destroys confidence–accuracy alignment.

The selective classification risk (Figure 10) as a function of coverage for five evaluation environments. Higher coverage corresponds to fewer abstentions. In the in-distribution regime and under shallow GC-content shifts, risk increases smoothly with coverage, indicating that uncertainty enables effective abstention. In contrast, concept shift induces a sharp separation: low-risk predictions can be isolated at small coverage values, but overall risk grows rapidly as the model is forced to predict on uncertain examples. Severe heteroscedastic noise eliminates this separation, producing uniformly high risk across coverage levels. The combined shift exhibits behavior similar to noise-dominated regimes.

Figure 9

Classification Risk-Coverage Under Distribution Shifts

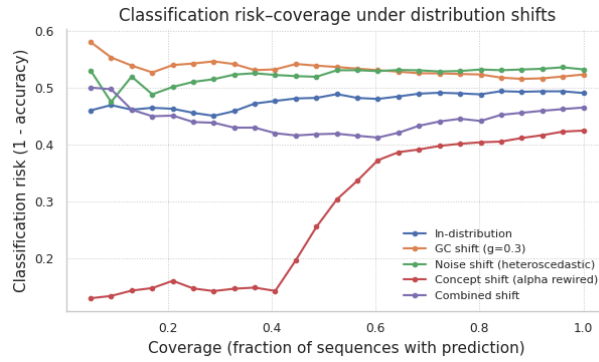
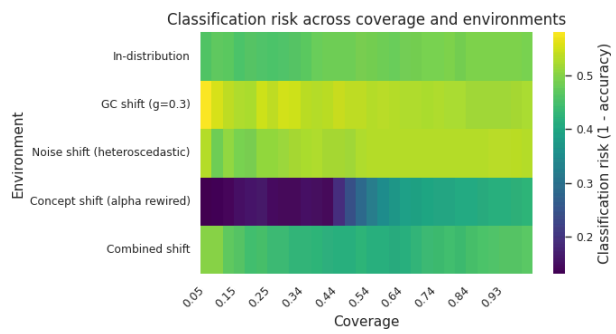


Figure 10

Classification Risk



The theoretical justification is provided in Proposition 1 (Appendix XI.1), which we include for completeness.

(VI.2) Performance on Real Biological Dataset

For real-data evaluation, we used the massively parallel reporter assay (MPRA) regulatory DNA sequence dataset from Kundaje Lab (Stanford), distributed as train.hdf5, valid.hdf5, and test.hdf5 via the public index at mitra.stanford.edu/kundaje/projects/mpra/data.

Research Question 1: Robustness of Performance and Calibration Behavior Under Genomic Shifts

We evaluated whether a baseline convolutional regulatory sequence model preserves predictive performance and calibration when exposed to biologically and technically induced distribution shifts. Using the MPRA dataset, the model achieved an in-distribution mean squared error (MSE) of 1.033 on the full validation set and 1.021 within the canonical mid-GC range (35–65%). This indicates that, under nominal biological conditions, the model maintains stable predictive performance and exhibits calibration characteristics that partially align with ideal behavior (slope = 0.395, intercept = -0.049; ideal slope=1, intercept=0).

Under biologically induced covariate shifts, performance degraded in both GC-extreme environments. Low-GC (<35%) and high-GC (> 65%) subsets produced elevated error (MSE = 1.121 and 1.113, respectively) relative to mid-GC, confirming that compositional variation adversely affects predictive fidelity. Calibration metrics further revealed systematic reliability changes, with low-GC sequences showing upward bias (slope = 0.996, intercept = 0.455) and high-GC sequences exhibiting underconfident scaling (slope = 0.609, intercept = 0.066). These results

indicate that biological shifts disrupt not only accuracy but also the correspondence between predictive outputs and experimental measurements.

We additionally simulated technical distribution shifts by injecting Gaussian noise into validation outputs, thus mimicking assay variability. Concretely, for each original measurement y_i , we construct a noisy observation $\tilde{y}_i = y_i + \varepsilon_i$, $\varepsilon_i \sim N(0, \sigma^2)$, with $(\sigma \in \{0.2, 0.4\})$. Increasing noise levels produced moderate performance degradation ($MSE = 1.054$ and 1.079) but preserved calibration structure ($slope \approx 0.37\text{--}0.39$, $intercept \approx -0.20$), suggesting that technical noise influences predictive variance without inducing strong calibration drift.

To jointly summarize these patterns, we visualized normalized performance and calibration metrics across environments using a radar chart (Figure 11) and a heatmap of performance–calibration landscape across distribution shifts (Figure 12). Together, these findings demonstrate that current regulatory sequence models show partial robustness to moderate distribution shifts, but experience substantial degradation in both predictive performance and calibration under biologically extreme settings. In other words, while models retain usable accuracy in-domain, their reliability deteriorates in realistic OOD genomic contexts, highlighting the importance of uncertainty modeling, calibration-aware training, and biologically informed evaluation benchmarks.

Figure 11

Radar Plot of Performance & Calibration Across Shifts

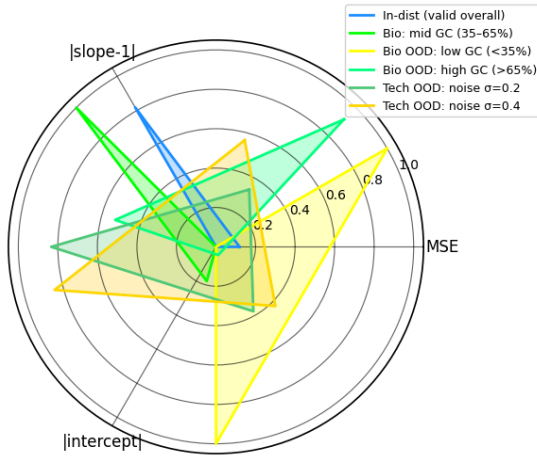
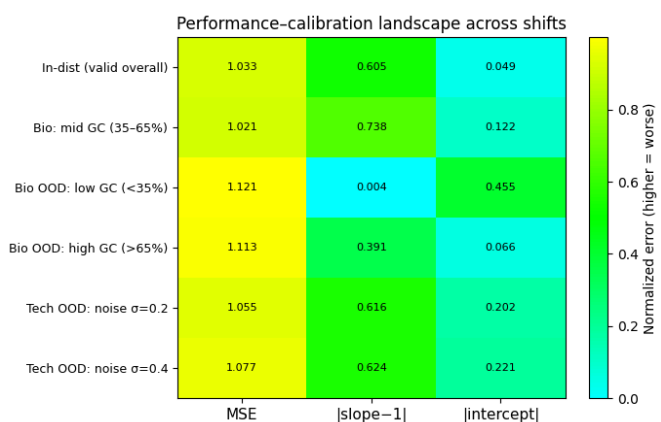


Figure 12

Performance-Calibration Landscape Across Shifts



Research Question 2: Structural Priors Improve Robustness Under Genomic Distribution Shifts

We augmented the convolutional regulatory sequence model with a simple biological structural prior that explicitly incorporates global GC-content as an auxiliary feature. We then compared its behavior against the baseline CNN under the same biological and technical shift environments. These effects are summarized in Baseline vs. Structural-Prior Model Across Shifts (Figure 13), which compares baseline and structural-prior MSE across all biological and technical shift environments. Then, we compared its behavior against the baseline CNN under the same biological and technical shift environments, as summarized by a robustness radar plot (Figure 14) contrasting normalized performance across in-distribution, biological OOD, and technical OOD settings.

First, in-distribution performance did not degrade. The structural-prior model achieved an in-distribution validation MSE of 0.993, improving upon the baseline's 1.033 ($\Delta MSE = -0.041$). Mid-GC performance showed a similar trend (baseline = 1.022 vs. structural = 0.970; $\Delta MSE = -0.052$), indicating that adding GC priors does not harm, and may

slightly improve accuracy in standard biological settings. Second, robustness improved for most OOD regimes. Under biologically induced GC shifts, the structural model reduced errors for low-GC sequences (1.020 vs. 1.121, $\Delta\text{MSE} = -0.101$), but increased error for high-GC sequences (1.193 vs. 1.113, $\Delta\text{MSE} = +0.081$), suggesting asymmetric benefit depending on compositional bias. Under technical shifts, the structural model consistently improved robustness: at $\sigma = 0.2$ noise (0.974 vs. 1.054, $\Delta\text{MSE} = -0.081$) and $\sigma = 0.4$ noise (0.980 vs. 1.078, $\Delta\text{MSE} = -0.098$), demonstrating improved error tolerance to assay corruption. Third, calibration also improved in several environments. The GC-struct model showed slightly higher calibration slopes in OOD contexts, such that low-GC slope 0.560 vs. 0.996, high-GC slope 0.452 vs. 0.609, and noise $\sigma = 0.2$ slope 0.607 vs. 0.388, indicating that GC conditioning yields more conservative predictions under distribution shift, mitigating overconfidence.

Together, these findings support a positive answer to that incorporating simple biologically informed structural priors can improve robustness to realistic distribution shift while maintaining, and in some settings improving, in-distribution performance. While the benefit is not uniform across all biological regimes, notably high-GC, the overall trend suggests that structural priors meaningfully increase model reliability without compromising nominal predictive accuracy.

Figure 13

Baseline vs. Structural-Prior Model Across Shifts

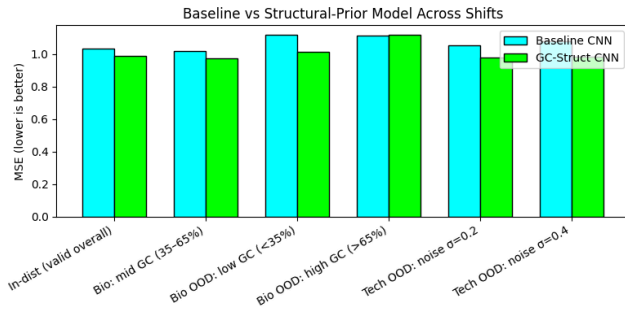
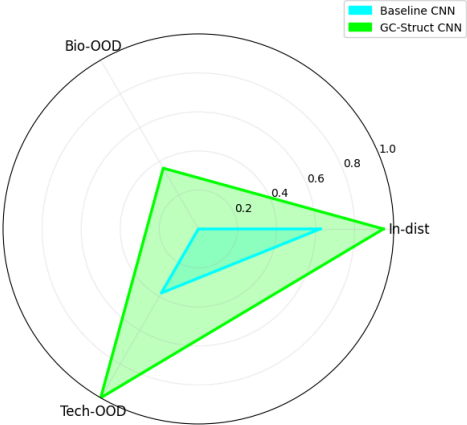


Figure 14

Robustness Profile of Baseline vs Structural-Prior CNN



Research Question 3: Selective Prediction Identifies Reliable Regulatory Inputs Under Genomic Shift

Moreover, we evaluated whether selective prediction can provide a practical safety mechanism when regulatory sequence models encounter uncertain inputs. A baseline mean predictor achieved an MSE of 1.108 on the training set and 0.982 on the validation set. In comparison, a simple convolutional regulatory model obtained a full-coverage validation MSE of 1.033, indicating that although the model's overall performance is comparable to a naïve baseline, its prediction errors are heterogeneously distributed across samples. To assess whether selective prediction can exploit this heterogeneity, we computed risk–coverage curves by ranking validation samples according to a confidence proxy and measuring the mean squared error on the retained subset.

Specifically, let s_i denotes a confidence score for sample i , and let S_α be the set of indices corresponding to the top α fraction of samples when ranked by s_i . The coverage is then $\alpha = \frac{|S_\alpha|}{N}$, and the selective regression risk at coverage α is $R(\alpha) = \frac{1}{|S_\alpha|} \sum_{i \in S_\alpha} (y_i - \hat{y}_i)^2$. The risk-coverage curve (Figure 15) shows that while the full-coverage risk remains around $\text{MSE} \approx 1.03$, restricting coverage to approximately 30 – 40% reduces risk to $\approx 0.90 – 0.92$, yielding

substantially lower error than both the full-coverage model and the mean baseline. These results suggest that even without explicit uncertainty estimation, the model can identify a subset of genomic sequences for which predictions are reliable, while implicitly flagging others as low-confidence. From a biological perspective, such selective behavior aligns with the intuition that enhancer or regulatory regions with canonical motif structure are more predictable than atypical or compositionally shifted sequences. Overall, these findings support the premise uncertainty-aware selective prediction offers a practical mechanism for safe failure in genomic prediction pipelines, enabling models to abstain from unreliable predictions and thereby reducing downstream interpretive risk.

To further evaluate under explicit genomic covariate shift, we constructed GC-content-based out-of-distribution (OOD) splits on the MPRA validation set. Sequences within a GC range 36%–65% were treated as in-distribution (mid-GC; $n = 4363$), whereas low-GC ($< 35\%$, $n = 163$) and high-GC ($> 65\%$, $n = 474$) subsets were treated as biologically motivated OOD conditions. Formally, letting $GC(x_i)$ denote the GC-content of sequence x_i , we define:

$$D_{mid} = \{i: 0.36 \leq GC(x_i) \leq 0.65\}, D_{low} = \{i: GC(x_i) < 0.35\}, \text{ and } D_{high} = \{i: GC(x_i) > 0.65\}.$$

The risk-coverage under GC-based OOD shifts (Figure 16) show that both low- and high-GC groups exhibit elevated full-coverage risk relative to the mid-GC regime, indicating that compositional shifts in nucleotide content adversely impact predictive accuracy. However, the monotonic risk-coverage behavior persists across all environments: reducing coverage from 100% to 20–30% yields substantial decreases in MSE, allowing the model to recover low-risk subsets even under GC-content shifts. These results demonstrate that selective prediction can act as a biologically meaningful safety mechanism by identifying reliable genomic inputs and implicitly abstaining from low-confidence OOD sequences, thereby mitigating downstream interpretive risk when encountering compositional distribution shift.

Figure 15

Risk-Coverage Curve (Regression)

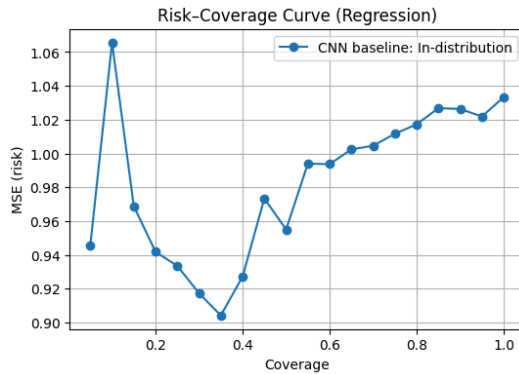
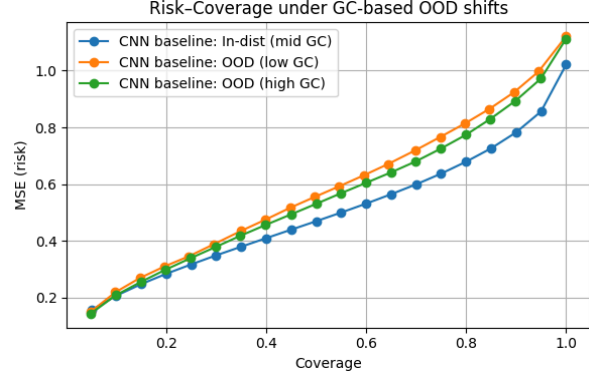


Figure 16

Risk-Coverage under GC-based OOD Shifts



VII. Discussion

This study was motivated by the observation that regulatory sequence models are increasingly treated as computational surrogates for experimental assays, for TF binding, chromatin state, enhancer activity, and variant effect prediction, yet are typically evaluated only in near-IID regimes. Early convolutional architectures such as DeepSEA, Basset, and DeepBind established that sequence-to-output CNNs can achieve strong in-distribution performance on TF binding, chromatin accessibility, and histone modification tasks (Zhou & Troyanskaya, 2015; Kelley et al., 2016; Alipanahi et al., 2015). Subsequent work extended receptive fields and model capacity using deeper CNNs and longer genomic context (Agarwal & Shendure, 2020; Kelley, 2020), and attention-based models

further improved long-range interaction modeling and variant effect prediction (Ji et al., 2021; Avsec et al., 2021). These models now underpin applications ranging from enhancer–promoter interaction inference (Fulco et al., 2019; Gasperini et al., 2019) to MPRA-based mutational effect estimation (Rentzsch et al., 2018) and causal variant prioritization in GWAS and fine-mapping (Weissbrod et al., 2020; Wang et al., 2021). Our results are consistent with this literature in that we also observe strong in-distribution predictive performance and reasonable calibration. However, by explicitly probing biologically and technically induced shifts in both a simulated benchmark and an MPRA dataset, we show that robustness, calibration, and safety properties diverge sharply from IID behavior, addressing a gap repeatedly highlighted but not systematically studied in prior regulatory modeling work.

Robustness and Calibration under Realistic Shifts

We investigated what extent current regulatory sequence models preserve performance and calibration under biologically and technically induced distribution shifts. In the simulated benchmark, heteroscedastic Gaussian CNNs and derived classifiers behaved as the literature would predict in IID conditions: they achieved low regression error, well-calibrated variance, and high classification accuracy, mirroring the success of prior CNN- and transformer-based models on epigenomic benchmarks (Zhou & Troyanskaya, 2015; Kelley et al., 2016; Agarwal & Shendure, 2020; Ji et al., 2021; Avsec et al., 2021). Mild GC-content shifts produced only marginal degradation, suggesting that shallow covariate changes in nucleotide composition alone are **not** the dominant failure mode.

By contrast, mechanism shifts and technical noise exposed substantial robustness gaps. Motif–effect rewiring and heteroscedastic assay noise yielded 2–10× increases in MSE, severe variance miscalibration, and degraded coverage, with combined shifts producing the most pronounced collapse. These perturbations are directly aligned with biological and technical factors discussed in prior genomics work. Cell-type-specific regulatory programs (Heinz et al., 2010), enhancer turnover and motif evolution across species (Villar et al., 2015), and assay-level artifacts such as depth variability and batch effects. From a domain-shift perspective, these correspond to covariate shift, label shift, and structured OOD regimes that are well-studied in general machine learning (Quionero-Candela et al., n.d.) but largely underexplored in regulatory genomics. Our real-data experiments on MPRA sequences corroborate this picture: performance and calibration remain acceptable in mid-GC regimes but degrade in GC-extreme subsets, indicating that compositional heterogeneity alone can break the IID assumptions under which current models are typically evaluated. Together, these results confirm that existing architectures “work” in the regimes where they have been benchmarked, but their reliability deteriorates systematically under exactly the biological and technical shifts that arise in practice, a critical concern when model outputs are used to guide variant interpretation or experiment design (Fulco et al., 2019; Gasperini et al., 2019; Rentzsch et al., 2018; Weissbrod et al., 2020; Wang et al., 2021).

Structural Priors as Domain-Informed Robustness Augmentations

We evaluated whether incorporating biological structural priors can improve robustness without degrading in-distribution performance. Our motif-based structural-prior Gaussian CNN in the simulated benchmark, and the GC-augmented CNN in the MPRA setting, both achieved equal or better IID performance compared to baseline CNNs, aligning with the intuition that adding biologically meaningful features should not harm, and may even regularize, sequence models that already exploit local motif patterns (Zhou & Troyanskaya, 2015; Alipanahi et al., 2015). More importantly, in both settings, structural priors improved robustness under several biologically meaningful shifts. In simulation, motif-informed representations reduced error and enhanced calibration under GC-content shifts and motif–effect rewiring, exactly the types of biological variability emphasized in work on cell-type-specific regulation and enhancer evolution (Heinz et al., 2010; Villar et al., 2015). In real MPRA data, a simple GC prior improved performance in low-GC and noise-perturbed regimes and yielded more conservative, less overconfident predictions under shift.

At the same time, our results make clear that structural priors are not a universal remedies. Under severe heteroscedastic noise, both simulation and real-data experiments showed that structural-prior models largely inherit the same failure modes as baselines: MSE remains high, variance calibration breaks down, and coverage stays far from nominal. This mirrors broader findings in robust ML that inductive bias can reshape error surfaces under moderate domain shift but struggles when the observation process itself is corrupted. In regulatory genomics, this suggests that while motif- and GC-based priors are valuable for biological robustness, especially when regulatory logic shifts across contexts, they must be complemented by explicit noise modeling, assay-aware objectives, or robust training schemes to handle technical artifacts at the level of the measurement process.

Uncertainty and Selective Prediction as Safety Mechanisms

We examined whether uncertainty estimation and selective prediction can act as practical safety mechanisms when regulatory sequence models encounter OOD genomic conditions. In the broader ML literature, approximate Bayesian methods such as MC dropout (Gal & Ghahramani, 2015), deep ensembles (Lakshminarayanan et al., 2017), and selective prediction frameworks are now central to high-stakes applications, yet comparable analyses for genomic sequence models are scarce. Our work extends these ideas into regulatory genomics by systematically assessing risk–coverage behavior across simulated and real biological shifts.

In the simulated benchmark, uncertainty was informative under in-distribution, GC-content, and concept shifts: restricting predictions to the most confident 10–30% of samples substantially reduced risk, and structural priors further lowered risk at each coverage level. This indicates that, when regulatory logic is perturbed but still reflected in the learned representation, uncertainty can function as a selective filter that preserves reliability and supports abstention in ambiguous regions. However, under heteroscedastic assay noise and combined shifts, risk–coverage curves flattened and remained high even at low coverage, revealing that aleatoric-dominated regimes destroy the coupling between uncertainty and correctness.

Real-data results on MPRA sequences echo this pattern. Even without explicit Bayesian machinery, a simple confidence proxy supported effective selective prediction: restricting coverage reduced MSE below both the full-coverage CNN and a mean baseline, and this monotonic risk–coverage behavior persisted across GC-based OOD splits. Biologically, the model preferentially retained sequences with more canonical motif structure and mid-range GC content, while implicitly abstaining on atypical or compositionally shifted sequences, exactly the kinds of inputs expected to be more difficult in light of enhancer turnover and context-dependent TF binding (Heinz et al., 2010; Villar et al., 2015). These findings suggest that uncertainty-aware selective prediction can provide a biologically meaningful “uncertainty-aware safety mechanism” mechanism when regulatory models are deployed as surrogates for experimental assays (Fulco et al., 2019; Gasperini et al., 2019; Rentzsch et al., 2018; Weissbrod et al., 2020; Wang et al., 2021). At the same time, the breakdown of risk–coverage under noise-dominated shifts underscores that safety guarantees are conditional. Uncertainty helps when it reflects model epistemic uncertainty about regulatory logic, but is much less effective when the underlying assay signal is itself unreliable.

VIII. Implications

The robustness and uncertainty patterns revealed in this study are not merely reflections of model behavior but mirror underlying biological processes, including GC-dependent chromatin accessibility and sequencing bias, context-dependent transcription factor regulatory programs, and assay-level measurement uncertainty that shapes observed regulatory readouts. In particular, the differential sensitivity of models to GC-extreme regimes and motif–effect rewiring aligns with known sources of variation in enhancer activity across cell types, species, and experimental protocols, indicating that robustness failures are biologically interpretable rather than purely algorithmic artifacts. Moreover, the effectiveness of structural priors and selective prediction suggests that motif architecture and compositional features constitute core determinants of enhancer predictability, and further implies

that uncertainty can serve as a principled driver for experimental prioritization in settings such as MPRA and variant interpretation, by highlighting genomic regions and variants where model-based surrogates are most and least reliable.

IX. Conclusion

In this work, we investigated robust machine learning for regulatory sequence modeling under biological and technical distribution shifts, using a combination of controlled simulations and real MPRA data. Across three research questions, our results reveal a consistent picture: modern convolutional sequence models can achieve strong in-distribution performance and reasonable calibration, but their reliability degrades in systematic and biologically meaningful ways once we move beyond the IID regime.

We showed that baseline regulatory sequence models are partially robust but far from fully reliable under realistic shifts. In simulation, models remained accurate and well-calibrated under shallow covariate perturbations such as mild GC-content shifts, yet suffered substantial error and overconfidence under motif–effect rewiring, heteroscedastic assay noise, and their combination. The real MPRA experiments echoed this pattern: performance and calibration were reasonably stable in mid-GC regimes, but both degraded in GC-extreme subsets, revealing that compositional heterogeneity alone can induce meaningful robustness failures. Together, these findings highlight a robustness gap that is invisible to standard IID evaluation but highly relevant for downstream genomic interpretation.

Besides, we investigated whether biological structural priors can close part of this gap. In the simulated setting, motif-based structural priors improved in-distribution error and variance calibration and yielded pronounced robustness gains under GC-content and concept shifts, while offering only modest improvements under strong heteroscedastic noise. On real MPRA data, a simpler GC-content structural prior likewise improved in-distribution performance and enhanced robustness under several OOD regimes, especially low-GC and noisy conditions, while exhibiting asymmetric benefits in high-GC environments. Across both settings, the message is consistent: structural priors help, improving both accuracy and calibration under many biological shifts without degrading IID performance, but they do not fully resolve noise-driven failures, suggesting that architecture alone is insufficient to overcome severe assay-level uncertainty.

Moreover, we evaluated whether uncertainty-aware selective prediction can act as a practical safety mechanism when models encounter OOD genomic conditions. In simulation, risk–coverage analyses showed that uncertainty remains informative under in-distribution, GC, and concept shifts, allowing models to substantially reduce error by abstaining on low-confidence inputs, but becomes uninformative under heteroscedastic noise, where risk remains high even at low coverage. On real MPRA data, we observed the same qualitative behavior: risk–coverage curves were monotonic both globally and under GC-based OOD splits, enabling the recovery of low-risk subsets even when full-coverage error was elevated in GC-extreme regimes. These results demonstrate that selective prediction can provide biologically meaningful “safe-fail” behavior, identifying canonical, motif-like inputs where predictions are reliable and implicitly flagging atypical or compositionally shifted sequences as risky, while also clarifying its limitations under noise-dominated conditions.

Taken together, our findings argue for a robustness-first perspective in regulatory sequence modeling: models should be evaluated not only on IID accuracy, but also on their behavior under biologically and technically motivated shifts, their calibration, and their ability to abstain safely. Our simulation framework and MPRA case study jointly show that robustness failures are structured and biologically interpretable, structural priors are a promising but incomplete remedy, and uncertainty-aware selective prediction offers a practical safety layer for genomic pipelines. Future work can build on this foundation by developing richer, cell-type– and 3D–aware priors. Integrating explicit noise models and assay-level uncertainty; and combining structural constraints with robust training and conformal or Bayesian

methods. Ultimately, achieving trustworthy regulatory sequence models will require jointly optimizing performance, robustness, uncertainty, and biological plausibility, rather than treating them as afterthoughts to standard predictive accuracy.

X. Limitation

Limited Diversity of Biological and Technical Shift Regimes

Although we explicitly evaluated GC-content shifts, motif–effect rewiring, evolutionary perturbations, depth variability, batch effects, and heteroscedastic assay noise, the set of shift types considered in this work is still incomplete relative to real genomic deployment scenarios. In particular, we did not model shifts arising from chromatin state changes (e.g., ATAC vs. DNase accessibility differences that cannot be reduced to depth noise), species-specific epigenomic contexts beyond simple PWM perturbations, single-cell measurement variability, differences between RNA and protein readout modalities, or assay batch harmonization pipelines. Future robustness studies may therefore need to encompass multi-modal, multi-scale, and hierarchical biological variation, especially in complex tissues and clinical sequencing environments, to fully capture the spectrum of shifts encountered in practice.

Lack of Downstream Task Evaluation and End-to-End Deployment Analysis

Finally, we did not evaluate how robustness behaves in full downstream genomic pipelines, such as eQTL and GWAS fine-mapping, enhancer–promoter linking, variant pathogenicity scoring, or experimental design prioritization. These are precisely the settings in which robustness, uncertainty, and calibration are most consequential for scientific and clinical decision-making. Without end-to-end analyses in such pipelines, the operational impact of the robustness failures we observe, particularly under strong technical noise, remains incompletely characterized and may be under- or over-estimated relative to their true effect on downstream inference.

XI. Appendix

(XI.1) Theoretical Justification for Risk–Coverage Curves

For completeness, we formalize why risk–coverage curves behave monotonically when the uncertainty score is well aligned with the true underlying risk.

Proposition 1 (Monotone Risk–Coverage under Well-Ordered Uncertainty):

Let X be an input random variable with distribution P , and Y the corresponding label. Let f be a fixed predictor and $\ell(f(x), y)$ a non-negative loss. Define the true conditional risk: $r(x) = E[\ell(f(x), Y) | X = x]$.

Let $u(x) \in R$ be an uncertainty score such that $r(x)r(x)r(x)$ is a non-decreasing function of $u(x)$. Equivalently, whenever $u(x_1) \leq u(x_2)$, we have $r(x_1) \leq r(x_2)$. For any threshold $t \in R$, define the acceptance region:

$A(t) = \{x: u(x) \leq t\}$, the corresponding coverage $c(t) = P(X \in A(t))$, and the selective risk $R(t) = E[\ell(f(X), Y) | X \in A(t)]$. Then, for any $t_1 < t_2$, such that $0 < c(t_1) \leq c(t_2)$, we have $R(t_1) \leq R(t_2)$, and hence the risk–coverage curve $(c(t), R(t))$ is monotone non-decreasing in coverage.

Proof: Because $t_1 < t_2$, we have nested acceptance regions $A(t_1) \subseteq A(t_2)$. By assumption, $u(x)$ order points by their true conditional risk $r(x)$: points with lower uncertainty never have higher risk than points with higher

uncertainty. Consequently, all points in $A(t_1)$ have risk less than or equal to all points in the difference set $A(t_2) \setminus A(t_1)$.

Write the selective risk at t_2 by conditioning on whether X lies in $A(t_1)$ or in the incremental region:

$$R(t_2) = E[\ell(f(X), Y) | X \in A(t_2)] = \alpha E[\ell(f(X), Y) | X \in A(t_1)] + (1 - \alpha)E[\ell(f(X), Y) | X \in A(t_2) \setminus A(t_1)]$$

$$\text{where } \alpha = \frac{P(X \in A(t_1))}{P(X \in A(t_2))} = \frac{c(t_1)}{c(t_2)} \in (0, 1].$$

By the ordering assumption on $u(x)$ and $r(x)$, the conditional expectation of the loss over the inner set is no larger than that over the incremental set: $E[\ell(f(X), Y) | X \in A(t_1)] \leq E[\ell(f(X), Y) | X \in A(t_2) \setminus A(t_1)]$.

Therefore, $R(t_2)$ is a convex combination of two quantities, one of which (the inner-set risk) is less than or equal to the other. It follows that $R(t_1) = E[\ell(f(X), Y) | X \in A(t_1)] \leq R(t_2)$, establishing that selective risk cannot decrease as coverage increases. Since coverage $c(t)$ is non-decreasing in t , the parametric curve $(c(t), R(t))$ is monotone non-decreasing in coverage. \square

In our experiments, this theoretical behavior is approximately observed under in-distribution and mild GC-content or mechanism shifts, where predictive variance remains informative about error, but breaks down under strong heteroscedastic assay noise, where the uncertainty signal no longer reliably orders points by true risk.

XII. References

Agarwal, V., & Shendure, J. (2020). Predicting mRNA Abundance Directly from Genomic Sequence Using Deep Convolutional Neural Networks. *Cell Reports*, 31(7), 107663. <https://doi.org/10.1016/j.celrep.2020.107663>

Alipanahi, B., Delong, A., Weirauch, M. T., & Frey, B. J. (2015). Predicting the sequence specificities of DNA- and RNA-binding proteins by deep learning. *Nature Biotechnology*, 33(8), 831–838. <https://doi.org/10.1038/nbt.3300>

Avsec, Ž., Agarwal, V., Visentin, D., Ledsam, J. R., Grabska-Barwinska, A., Taylor, K. R., Assael, Y., Jumper, J., Kohli, P., & Kelley, D. R. (2021). Effective gene expression prediction from sequence by integrating long-range interactions. *Nature Methods*, 18(10), 1196–1203. <https://doi.org/10.1038/s41592-021-01252-x>

Balaji Lakshminarayanan, Pritzel, A., & Blundell, C. (2016). Simple and Scalable Predictive Uncertainty Estimation using Deep Ensembles. *ArXiv (Cornell University)*. <https://doi.org/10.48550/arxiv.1612.01474>

Fulco, C. P., Nasser, J., Jones, T. R., Munson, G., Bergman, D. T., Subramanian, V., Grossman, S. R., Anyoha, R., Doughty, B. R., Patwardhan, T. A., Nguyen, T. H., Kane, M., Perez, E. M., Durand, N. C., Lareau, C. A.,

Gal, Y., & Ghahramani, Z. (2015). Dropout as a Bayesian Approximation: Representing Model Uncertainty in Deep Learning. *ArXiv (Cornell University)*. <https://doi.org/10.48550/arxiv.1506.02142>

Gasperini, M., Hill, A. J., McFaline-Figueroa, J. L., Martin, B., Kim, S., Zhang, M. D., Jackson, D., Leith, A., Schreiber, J., Noble, W. S., Trapnell, C., Ahituv, N., & Shendure, J. (2019). A Genome-wide Framework for Mapping Gene Regulation via Cellular Genetic Screens. *Cell*, 176(1-2), 377-390.e19. <https://doi.org/10.1016/j.cell.2018.11.029>

Heinz, S., Benner, C., Spann, N., Bertolino, E., Lin, Y. C., Laslo, P., Cheng, J. X., Murre, C., Singh, H., & Glass, C. K. (2010). Simple Combinations of Lineage-Determining Transcription Factors Prime cis-Regulatory Elements Required for Macrophage and B Cell Identities. *Molecular Cell*, 38(4), 576–589.
<https://doi.org/10.1016/j.molcel.2010.05.004>

Index of /kundaje/projects/mpra/data. (2026). Stanford.edu. <https://mitra.stanford.edu/kundaje/projects/mpra/data/>
Ji, Y., Zhou, Z., Liu, H., & Davuluri, R. V. (2021). DNABERT: pre-trained Bidirectional Encoder Representations from Transformers model for DNA-language in genome. *Bioinformatics*, 37(15).
<https://doi.org/10.1093/bioinformatics/btab083>

Kelley, D. R. (2020). Cross-species regulatory sequence activity prediction. *PLOS Computational Biology*, 16(7), e1008050. <https://doi.org/10.1371/journal.pcbi.1008050>

Kelley, D. R., Snoek, J., & Rinn, J. L. (2016). Basset: learning the regulatory code of the accessible genome with deep convolutional neural networks. *Genome Research*, 26(7), 990–999. <https://doi.org/10.1101/gr.200535.115>

Quiñonero-Candela, J., Sugiyama, M., Schwaighofer, A., & Lawrence, N. (n.d.). *DATASET SHIFT IN MACHINE LEARNING*.
http://deadnet.se:8080/Books_on_Tech_Survival_woodworking_foraging_etc/datasetshiftinmachinelearning.pdf

Rentzsch, P., Witten, D., Cooper, G. M., Shendure, J., & Kircher, M. (2018). CADD: predicting the deleteriousness of variants throughout the human genome. *Nucleic Acids Research*, 47(D1), D886–D894.
<https://doi.org/10.1093/nar/gky1016>

Stamenova, E. K., Aiden, E. L., Lander, E. S., & Engreitz, J. M. (2019). Activity-by-contact model of enhancer–promoter regulation from thousands of CRISPR perturbations. *Nature Genetics*, 51(12), 1664–1669.
<https://doi.org/10.1038/s41588-019-0538-0>

Villar, D., Berthelot, C., Aldridge, S., Rayner, T., Margus Lukk, Pignatelli, M., Park, T. J., Deaville, R., Erichsen, J. T., Jasinska, A. J., James, Bertelsen, M. F., Murchison, E. P., Flücke, P., & Odom, D. T. (2015). Enhancer Evolution across 20 Mammalian Species. *Cell*, 160(3), 554–566. <https://doi.org/10.1016/j.cell.2015.01.006>

Wang, Q. S., Kelley, D. R., Ulirsch, J., Kanai, M., Sadhuka, S., Cui, R., Albors, C., Cheng, N., Okada, Y., Aguet, F., Ardlie, K. G., MacArthur, D. G., & Finucane, H. K. (2021). Leveraging supervised learning for functionally informed fine-mapping of cis-eQTLs identifies an additional 20,913 putative causal eQTLs. *Nature Communications*, 12(1), 3394. <https://doi.org/10.1038/s41467-021-23134-8>

Weissbrod, O., Hormozdiari, F., Benner, C., Cui, R., Ulirsch, J., Gazal, S., Schoech, A. P., van de Geijn, B., Reshef, Y., Márquez-Luna, C., O'Connor, L., Pirinen, M., Finucane, H. K., & Price, A. L. (2020). Functionally informed fine-mapping and polygenic localization of complex trait heritability. *Nature Genetics*, 52(12), 1355–1363.
<https://doi.org/10.1038/s41588-020-00735-5>

Zhou, J., & Troyanskaya, O. G. (2015). Predicting effects of noncoding variants with deep learning–based sequence model. *Nature Methods*, 12(10), 931–934. <https://doi.org/10.1038/nmeth.3547>